ORNL/TM-2018/766

FY18Q1 Quarterly Report: Radiation Enhanced Diffusion of Ag, Ag-Pd, Eu, and Sr in Neutron Irradiated PyC/SiC Diffusion Couples

Tyler J. Gerczak
Anne A. Campbell
John D. Hunn
Brian C. Jolly
Austin T. Schumacher

January 2018

OAK RIDGE NATIONAL LABORATORY
MANAGED BY UT-BATTELLE FOR THE US DEPARTMENT OF ENERGY

ORNL/TM-2018/766

Fusion and Materials for Nuclear Systems Division

FY18Q1 QUARTERLY REPORT: RADIATION ENHANCED DIFFUSION OF AG, AG-PD, EU, AND SR IN NEUTRON IRRADIATED PYC/SIC DIFFUSION COUPLES

Tyler J. Gerczak
Anne A. Campbell
John D. Hunn
Brian C. Jolly
Austin T. Schumacher

Date Published: January 2018

Prepared by
OAK RIDGE NATIONAL LABORATORY
Oak Ridge, TN 37831-6283
managed by
UT-BATTELLE, LLC
for the
US DEPARTMENT OF ENERGY
under contract DE-AC05-00OR22725

CONTENTS

LIST OF FIGURES

LIST OF TABLES

ACRONYMS

AGR	Advanced Gas Reactor (Fuel Development and Qualification Program)
AGR-1	First AGR fuel irradiation experiment
AGR-2	Second AGR fuel irradiation experiment
CGF	Coating gas fraction
CVD	Chemical vapor deposition
EBSD	Electron backscatter diffraction
FBCVD	Fluidized-bed chemical vapor deposition
IPF	Inverse pole figure
LIBS	Laser-induced-breakdown spectroscopy
MTS	Methyltrichlorosilane
NEUP	Nuclear Energy University Program
OPTAF	Optical anisotropy factor
PyC	Pyrolytic carbon or pyrocarbon
S-PyC	Support pyrocarbon
sccm	Standard cubic centimeters per minute
SiC	Silicon carbide (TRISO layer)
TGF	Total gas flow
TRISO	Tristructural-isotropic (coated particles)
UCO	mixed uranium carbide/uranium oxide (kernels)

ACKNOWLEDGMENTS

This research is being performed using funding received from the DOE Office of Nuclear Energy's Nuclear Energy University Program through a joint NEET/NEUP R&D with NSUF access award (Project 16-10764). Significant support for this work was provided by Victoria Cox, J. Travis Dixon, John Dyer, and Tom Geer.

ABSTRACT

Obtaining accurate diffusion kinetics in materials representative of those found in tristructural-isotopic (TRISO) coated particle fuel is needed to predict the diffusive release of the same fission products in reactor. Planar diffusion couples with representative pyrocarbon (PyC) and silicon carbide (SiC) layers are being produced using the same fluidized-bed chemical vapor deposition (FB-CVD) technology used to produce TRISO particles from the first irradiation experiment of the Advanced Gas Reactor Fuel Qualification and Development Program (AGR). The layer properties of the planar diffusion couples are tailored to meet the specified PyC density and microstructure of the SiC layer as defined by the AGR program. The influence of these variables on diffusion is also being explored by producing PyC and SiC variants. The pathway to producing the diffusion couples is discussed

1. INTRODUCTION

Planar pyrocarbon (PyC) and silicon carbide (SiC) diffusion couples are being fabricated to explore diffusion in various exposure conditions including high temperature and high temperature neutron irradiation environments. The PyC/SiC construction serves to represent the diffusion pathway for fission product species in tristructural-isotropic (TRISO) coated particle fuel and allows for diffusion analysis in representative systems to be obtained. Previous efforts focused on initiating process development to identify the route to produce representative pyrocarbon (PyC) and silicon carbide (SiC) layered substrates for diffusion analysis. A summary of the previous results can be found in the report by Gerczak *et al*., "Progress on Fabrication of Planar Diffusion Couples with Representative TRISO PyC/SiC Microstructure" ORNL/TM-2017/704 [1]. The PyC/SiC samples are fabricated using a fluidized-bed chemical vapor deposition (FB-CVD) reactor by depositing the PyC/SiC layers on a 9-mm-diameter disk. The disk substrate is different from the coating approach of TRISO particles, which deposits the layers on spherical particles. Previous coating experience was utilized to select initial coating conditions to target specific layer properties, however the difference in geometry of the disk relative to the spherical TRISO particles led to a PyC/SiC coating microstructure which varied from previous experience. The observed variation is expected to be due to different fluidization behavior of the disks, and possibly from the effect of deposition on flat versus round surfaces. This report summarizes the work completed in FY18Q1 and focuses on refining the coating process to obtain PyC/SiC microstructures which meet the targeted properties for the three identified variants (Baseline, SiC Variant, PyC Variant).

2. FABRICATION OF PYC/SIC/S-PYC SAMPLES

The PyC/SiC sample fabrication process initiates with the deposition of a thin PyC layer on a 9-mm-diameter sapphire disk followed by successive deposition of the SiC layer and support PyC (S-PyC) layer which provides strength to the samples. The deposition conditions are varied to attain targeted properties of the PyC and SiC layers for each defined variant. A detailed description of the FB-CVD deposition process is found in reference [1]. Table 1 lists the targeted properties of the variants. The properties are derived from TRISO particle fuel properties from the first and second irradiation experiments (AGR-1 and AGR-2) of the Advanced Gas Reactor Fuel Qualification and Development Program [2–4]. SiC density and SiC microstructure are the primary targets for the three variants, however, PyC density and PyC anisotropy will be measured for the final samples. The PyC anisotropy will be reported in terms of the optical anisotropy factor (OPTAF). A systematic process to identify the necessary conditions to obtain ideal PyC densities for all three variants was demonstrated in the work prior to FY18Q1.

Table 1. Properties of AGR-2 UCO fuel variant and the three planar diffusion couple variants in this study.

		PyC Density	PyC Anisotropy	SiC Density	**SiC Grain Size**	
		(g/cm^3)	(OPTAF)[b]	(g/cm^3)	(major axis, μm)	(minor axis, μm)
AGR-2 UCO TRISO measured values[a] [2–4]		1.890±0.011	1.0236 ± 0.0008[c]	3.197±0.004	0.89±0.14	0.35±0.05
Targets	Baseline	1.85–1.95	≤1.03	≥3.19	0.75–1.03	0.30–0.40
	PyC Variant	>1.95	≤1.03	≥3.19	0.75–1.03	0.30–0.40
	SiC Variant	1.85–1.95	≤1.03	≥3.19	2.10–2.70	0.50–0.80

[a]values reported as mean±standard deviation
[b]OPTAF = (1+N)/(1-N), where N is the measured optical diattenuation of the PyC
[c]OPTAF of the inner pyrocarbon layer after SiC deposition

After the PyC/SiC/S-PyC layers are constructed, up to four samples, ~3 x 4–5 mm, are sectioned from each 9-mm-disk. Note that the length of the final sample size varies to allow for identification of each variant after irradiation and thermal exposure. The Baseline sample is 3 x 5 mm, the SiC Variant is 3 x 4.5 mm and the PyC Variant is 3 x 4 mm. After sectioning, the relevant fission product species are to be implanted into the PyC layer that has been tailored to meet a targeted density. Following implantation, a SiC seal coat is applied over the PyC/SiC/S-PyC sample via FB-CVD to create a self-contained system which contains the remaining fission product species during thermal exposure and neutron irradiation in the High Flux Isotope Reactor. Figure 1 shows a cross section of a PyC/SiC/S-PyC sample after SiC seal coating to provide context to the sample construction.

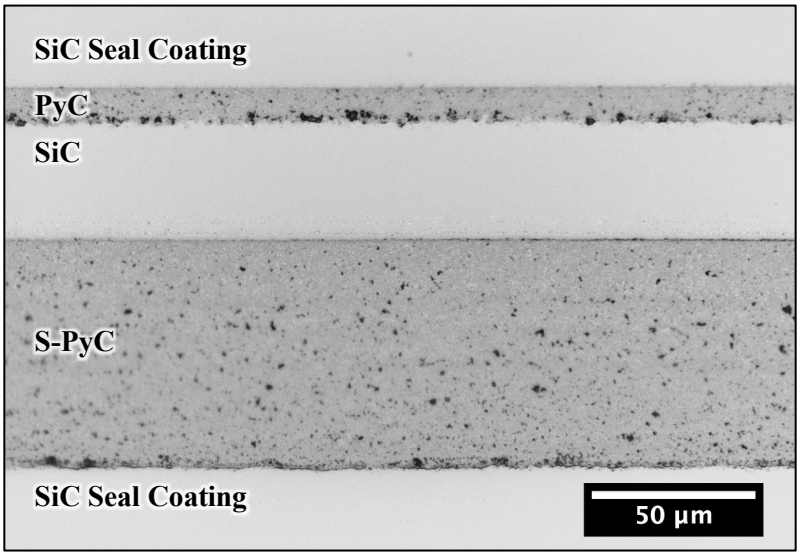

Figure 1. Optical micrograph of the PyC/SiC/S-PyC construction after SiC seal coating showing layer construction.

The PyC layer is deposited on the surface of the fluidized media by decomposition of the precursor gases, acetylene (C_2H_2) and propene (C_3H_6) with an Ar fluidization gas. Runs where only the PyC layer was deposited were completed to isolate the PyC layer and measure the density using a density column according to the previously defined procedure in AGR-CHAR-DAM-03 Rev. 4 [5]. Table 2 shows the PyC-only deposition run conditions and density measurements, while Figure 2 shows the density versus

deposition temperature for the associated runs. The density for DCCD-15I (1270 °C) is underestimated, as some fragments had densities higher than the density range of the column. This yielded a reported density which is not represntentative of the true average. The PyC deposition conditions for DCCD-15I will be repeated to improve the confidence of the density measurement at 1270 °C. A confirmatory run (DCCD-20I) was completed this quarter to establish the PyC deposition conditions for the Baseline and SiC Variants. The run, DCCD-20I confirmed PyC deposited at 1350 °C resulted in an appropriate PyC density centered around 1.90 g/cm^3. The target for the PyC Variant was >1.95 g/cm^3; however, to ensure significant variation in the PyC/SiC interface was present, an exaggerated PyC density of 2.00 g/cm^3 was sought. Based on the production curve, a density of ~2.00 g/cm^3 was attainable at target deposition temperatures of ~1300 °C. An interrupted PyC deposition and subsequent density analysis is planned to validate the PyC density deposited at 1300 °C.

Table 2. Coating conditions for confirmatory PyC only interrupted runs.

Run	Run Time	Temperature	Ar Fluid. Gas	C_2H_2	C_3H_6	CGF[a]	PyC Density[b] (g/cm^3)
DCCD-12I	4.9 min	1310 °C	4200	973	827	0.30	1.989±0.281
DCCD-13I	4.9 min	1310 °C	4200	973	827	0.30	1.973±0.069
DCCD-14I	4.3 min	1350 °C	4200	973	827	0.30	1.883±0.026
DCCD-15I	5.5 min	1270 °C	4200	973	827	0.30	2.011±0.002[c]
DCCD-16I	6.6 min	1390 °C	4200	973	827	0.30	1.754±0.038
DCCD-18I	4.5 min	1340 °C	4200	973	827	0.30	1.946±0.015
DCCD-20I	4.3 min	1350 °C	4200	973	827	0.30	1.907±0.024

All gas flow rates are in standard cubic centimeters per minute (sccm)
[a]Coating gas fraction (CGF) is defined as precursor gas flow divided by total gas flow (TGF)
[b]The ± values indicate one standard deviation in the distribution from the mean value.
[c]The density for DCCD-15I is underestimated.

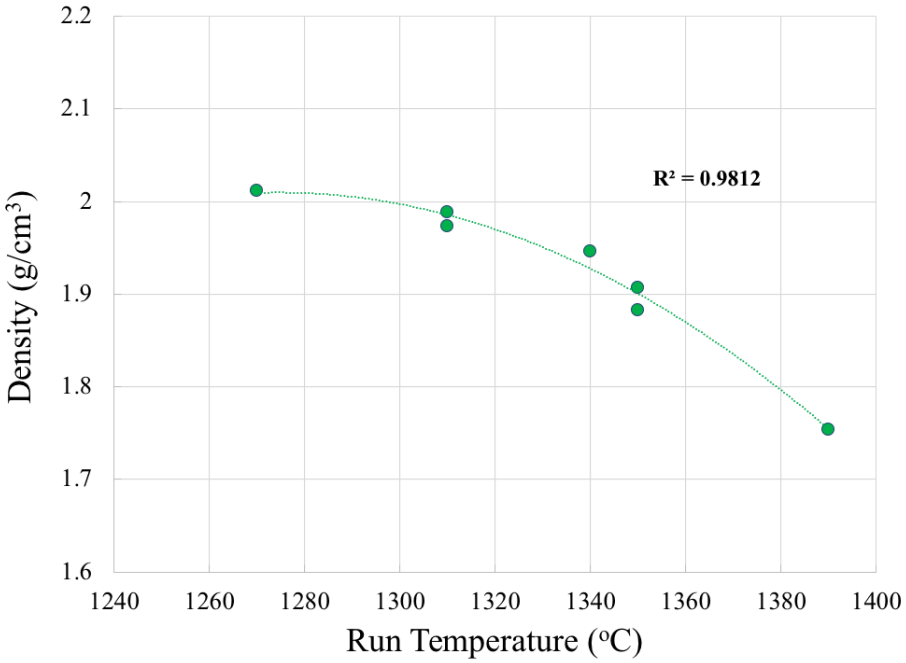

Figure 2. Density versus run temperature for confirmatory PyC-only interrupted runs.

Additional research and development efforts were needed to define the optimal SiC microstructures for each variant. Table 3 lists the conditions for SiC deposition on the 9-mm-disk substrates. The SiC layer is deposited via the decomposition of methyltrichlorosilane (MTS) and various fluidization gases can be used such as Ar and H_2. The impact of coating variables such as fluidization gas (Ar, Ar+H_2), bed deposition temperature, and coating gas fraction (CGF) on the resultant SiC microstructure for spherical particles has been determined from prior experience with FB-CVD coaters [6,7]. This insight has been used to direct deposition conditions to obtain the targeted SiC layer properties.

Table 3. Coating conditions for the full PyC/SiC/S-PyC coating runs.

Run	Layer	Run Time (min)	Temp. (°C)	Ar	H_2	C_2H_2	C_3H_6	CGF[a]	MTS used (g)
DCCD-02	PyC	2.8	1295	6300	-	1460	1240	0.3	-
	SiC	269	1425	3250	3250	-	-	0.015	180
	S-PyC	46	1320	6300	-	1460	1240	0.3	-
DCCD-03	PyC	2.8	1295	6300	-	1460	1240	0.3	-
	SiC	250	1425	3250	3250	-	-	0.016	181
	S-PyC	46	1320	6300	-	1460	1240	0.3	-
DCCD-04	PyC	2.8	1295	6300	-	1460	1240	0.0	-
	SiC	244	1425	3250	3250	-	-	0.017	182
	S-PyC	46	1320	6300	-	1460	1240	0.3	-
DCCD-06	PyC	3	1335	6300	-	1460	1240	0.3	-
	SiC	177	1425	3250	3250	-	-	0.023	180
	S-PyC	45	1320	6300	-	1460	1240	0.3	-
DCCD-17	PyC	4.43	1340	4200	-	973	827	0.3	-
	SiC	147	1500	-	7000	-	-	0.026	186
	S-PyC	46	1320	6300	-	1460	1240	0.3	-
DCCD-23	PyC	4.27	1350	4200	-	973	827	0.3	-
	SiC	195	1450	3250	3250	-	-	0.021	180
	S-PyC	46	1320	6300	-	1460	1240	0.3	-

DCCD-24	PyC	4.27	1350	4200	-	973	827	0.3	-
	SiC	201	1475	3250	3250	-	-	0.020	180
	S-PyC	46	1320	6300	-	1460	1240	0.3	-
DCCD-25	PyC	4.27	1350	4200	-	973	827	0.3	-
	SiC	67	1500	-	13000	-	-	.025	150
	S-PyC	46	1320	6300	-	1460	1240	0.3	-
DCCD-26	PyC	4.27	1350	4200	-	973	827	0.3	-
	SiC	80	1500	-	13000	-	-	0.021	150
	S-PyC	46	1320	6300	-	1460	1240	0.3	-
DCCD-27	PyC	5.06	1300	4200	-	973	827	0.3	-
	SiC	175	1450	3250	3250	-	-	0.023	180
	S-PyC	46	1320	6300	-	1460	1240	0.3	-
DCCD-28	PyC	4.27	1350	4200	-	973	827	0.3	-
	SiC	188	1550	3250	3250	-	-	0.022	180
	S-PyC	46	1320	6300	-	1460	1240	0.3	-
DCCD-29	PyC	4.27	1350	4200	-	973	827	0.3	-
	SiC	82	1550	-	13000	-	-	0.021	150
	S-PyC	46	1320	6300	-	1460	1240	0.3	-
DCCD-30	PyC	4.27	1350	4200	-	973	827	0.3	-
	SiC	182	1450	3250	3250	-	-	0.022	180
	S-PyC	46	1320	6300	-	1460	1240	0.3	-

All gas flow rates are in sccm

[a]Coating gas fraction (CGF) is defined as precursor gas flow divided by total gas flow (TGF)

Initial screening of the SiC layer from each run was performed by cross-sectioning and optical microscopy. Scanning electron microscopy (SEM) imaging was employed to provide general insight on the microstructure while a statistical measurement of the grain size was determined using electron backscatter diffraction (EBSD) techniques. This approach is identical to that used to measure the targeted grain sizes from AGR-1 and AGR-2 TRISO fuel particles [4].

2.1 DEVELOPMENT OF BASELINE AND PYC VARIANT SIC LAYER

The initial trial runs, DCCD-02 through DCCD-04, established full coating capability and started with coating conditions similar to those used to deposit the fine grain SiC microstructures from AGR-1 TRISO particles [6]. Initial analysis showed the SiC layer contained undesired features, likely porosity or grain structure susceptible to pull-out, throughout the layer. This is shown in the optical micrograph of Figure 3 which shows the non-ideal SiC microstructure. To remedy this, the CGF was increased from 0.015–0.017 to 0.023 to reduce the porosity/pull out observed in the SiC layer cross sections.

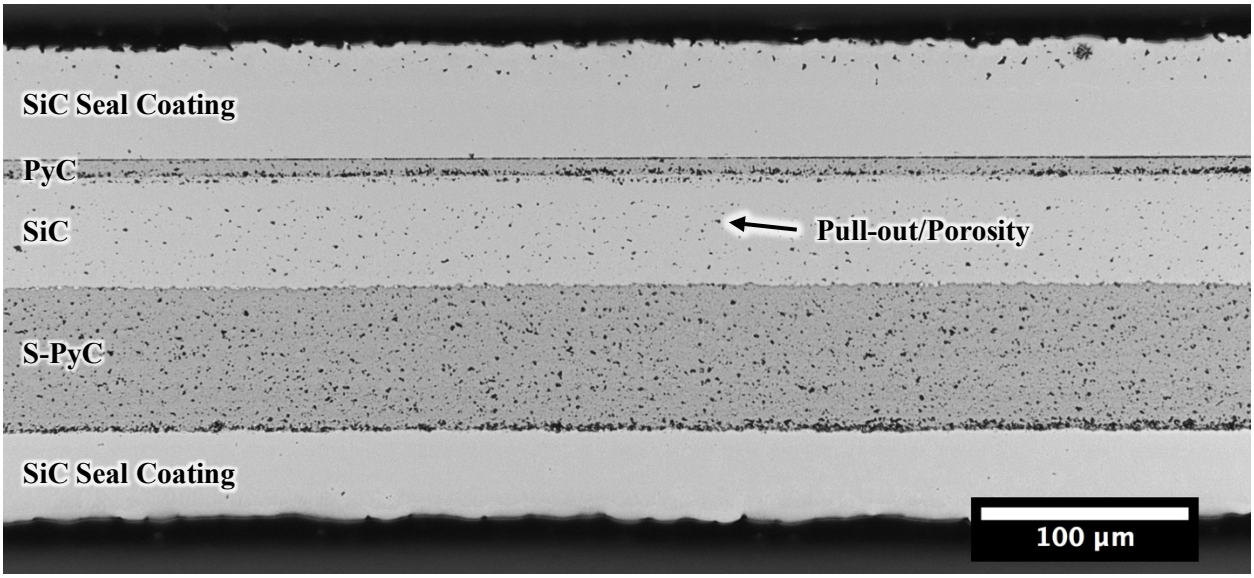

Figure 3. Optical micrograph of DCCD-04 (after seal coating) showing low-quality SiC with porosity/pull-out in SiC layer.

The subsequent run, DCCD-06, with increased CGF presented an improvement concerning the frequency of pores/pull-out in the SiC layer. EBSD analysis was employed to measure the SiC grain sizes from DCCD-06. Grain size is reported in major and minor axes based on the shape and size of an ellipse for each unique grain identified through EBSD analysis. Reporting grain size in this manner is ideal due to the non-equiaxed grain shape associated with the FB-CVD SiC deposition process [4]. Table 4 lists the major and minor axis lengths for the SiC and PyC Variant runs. A minimum of two samples were investigated per coating run for all reported EBSD results. The grain size is measured for the first 20 µm of the SiC layer as this is the depth that is relevant to diffusion analysis. While, DCCD-06 showed improved visual appearance, the average grain size was too small relative to the targeted grain size [1]. To increase the grain size, higher deposition temperatures were pursued. The run for DCCD-06 was deposited at 1425 °C, and the subsequent runs for DCCD-23 and DCCD-24 were deposited at 1450 °C and 1475 °C, respectively. The relatively-small increases in temperature were selected as a 24% increase in grain size was necessary to meet the targeted grain size.

Table 4. EBSD grain size measurements for Baseline and PyC Variant development.

Run	Variant	Major Axis (µm)[a]	Minor Axis (µm)[a]
Target	*Baseline/PyC*	*0.89±0.14*	*0.35±0.05*
DCCD-03	Baseline	1.05±0.26	0.41±0.09
DCCD-06	Baseline	0.67±0.13	0.25±0.04
DCCD-23	Baseline	0.85±0.33	0.30±0.08
DCCD-24	Baseline	1.03±0.38	0.41±0.11
DCCD-27	PyC	In Progress	In Progress
DCCD-30	Baseline	In Progress	In Progress

[a]The ± values indicate one standard deviation in the distribution from the mean value.

The resultant grain sizes for DCCD-23 and DCCD-24 yielded the expected increases in grain size relative to DCCD-06. Figure 4 shows a SEM backscatter electron (BSE) micrograph of a cross-section from

DCCDC-23 and inverse pole figure (IPF) map highlighting the fine-grain microstructure. The sample for DCCD-23 showed ideal microstructure as measured by EBSD that met the required targeted grain size. The deposition conditions for DCCD-23 were selected for Baseline and PyC production conditions.

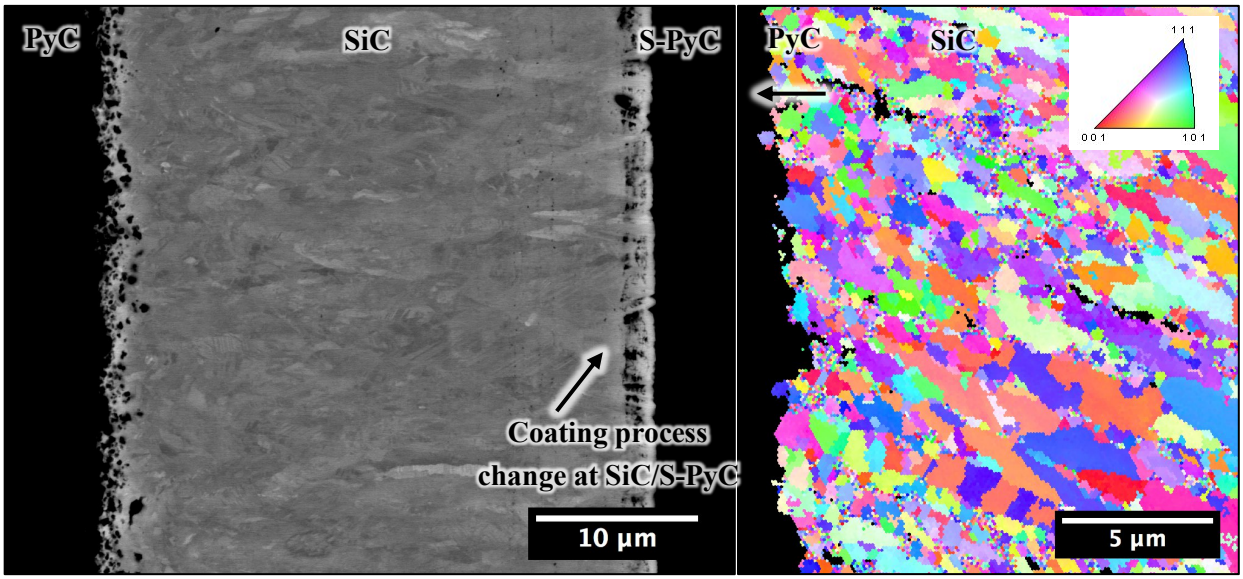

Figure 4. BSE micrograph and EBSD IPF map of the SiC layer from DCCD-23 highlighting the SiC microstructure of the Baseline and PyC Variant deposition conditions.

Also observed was a change in the coating process at the end of the SiC deposition. In Figure 4, the feature associated with the change in the coating process is observed ~30 µm from the PyC/SiC interface, the severity of the feature is exaggerated due to the brightness and contrast settings selected to expose the SiC microstructure in the BSE imaging mode. A higher magnification, secondary electron imaging (SEI) micrograph, which provides increase surface sensitivity relative to BSE, is shown in Figure 5 and suggests the SiC feature presents a local increase in porosity. The feature is not expected to impact the diffusion analysis as it is beyond the depth associated with diffusion depth profiling analysis and the excess thickness is needed to provide structural support. A speculation on the cause of the change in coating behavior is that a change in the flux of the decomposition products to the sample surface is occurring, as the total surface area in the bed increases with deposition time when a constant CGF is maintained. It is plausible that a critical point is reached in the latter half of the deposition resulting in a lower quality SiC similar to that observed with lower CGF for the initial deposition runs (DCCD-02–DCCD-04). This issue results in difficulty in controlling the SiC microstructure at the end of the deposition process only and at thicknesses where the SiC layer is being deposited for structural support.

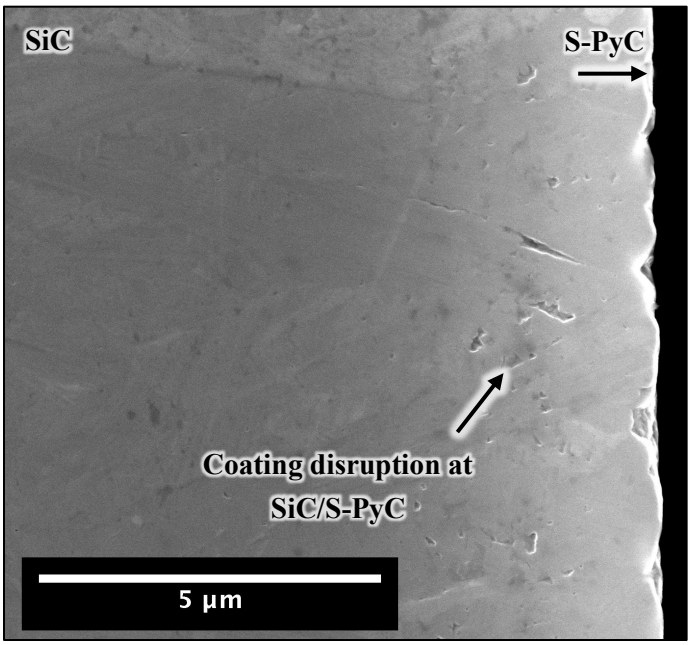

Figure 5. SEI image showing porosity associated with the change in the coating process at the SiC/S-PyC interface.

2.2 DEVELOPMENT OF SIC VARIANT SIC LAYER

The initial deposition conditions for the large-grain SiC Variant were selected based on AGR-1 coating approaches [6]. For the initial approaches the SiC Variant deposition used pure H_2 fluidization gas instead of Ar:H_2 like the Baseline and PyC Variants. The first run for the SiC Variant was DCCD-17. The microstructure for DCCD-17 showed significant porosity, Figure 6. The measured grain size was also more representative of the fine-grained Baseline and PyC Variant as reported in the EBSD grain size data for the SiC Variant in Table 5.

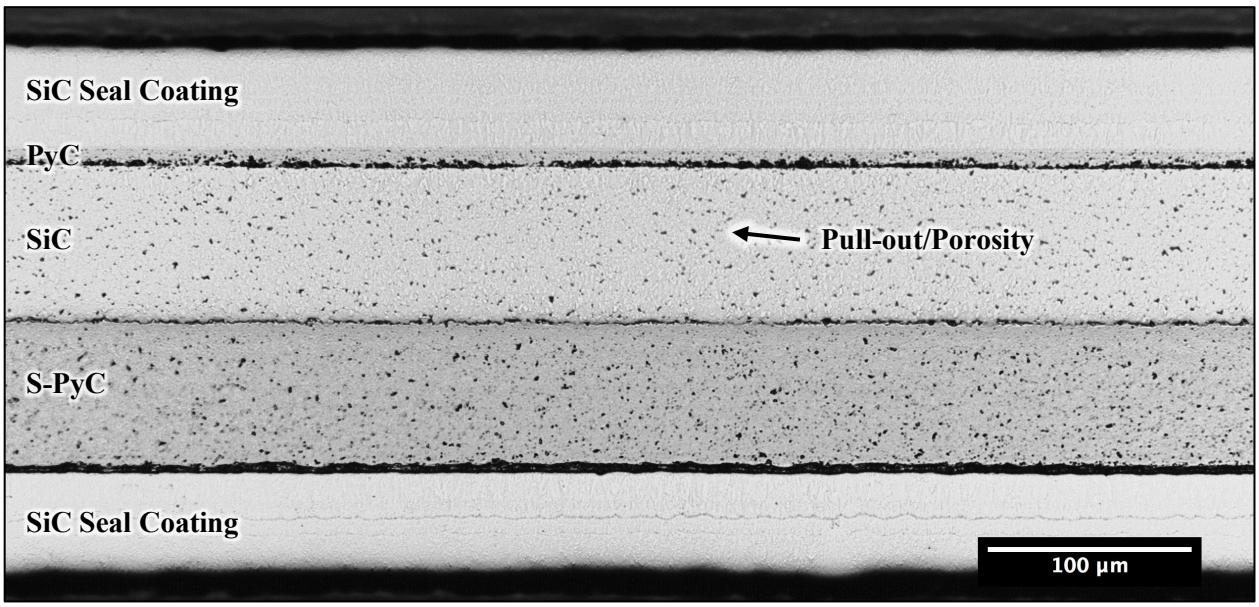

Figure 6. Optical micrograph of DCCD-17 (after seal coating) showing low-quality SiC with porosity/pull-out in SiC layer.

Table 5. EBSD grain size measurements for SiC Variant development.

Run	Variant	Major Axis (μm)[a]	Minor Axis (μm)[a]
Target	*SiC*	*2.39±0.24*	*0.71±0.05*
DCCD-17	SiC	0.82±0.24	0.38±0.13
DCCD-25	SiC	1.44±0.47	0.45±0.11
DCCD-26	SiC	1.65±0.54	0.50±0.16
DCCD-28	SiC	2.50±1.01	0.53±0.14
DCCD-29	SiC	1.84±0.77	0.44±0.11

[a]The ± values indicate one standard deviation in the distribution from the mean value.

The subsequent SiC Variant runs of DCCD-25 and DCCDC-26 explored increased TGFs (7000 to 13000 sccm for the fluidization gas) and varied CGFs. The SiC microstructure showed an increase in grain size relative to the measured grain size of DCCD-17 but were also below the targeted values for the SiC Variant, Table 5. The SiC layer also displayed some porosity/pull-out in the SiC layer but at a lower frequency than DCCD-17, as shown in Figure 7. The samples also showed an apparent reduction in grain size beyond the first 10-μm from the surface which coincided with the increase in pull-out/porosity; this suggests a possible deposition issue associated with the high TGF needed for the pure H_2 fluidization gas runs. However, the takeaway was that increased total gas flow led to improved grain sizes for DCCDC-25 and the reduction in CGF for DCCD-26 also moved the grain size toward the target goal.

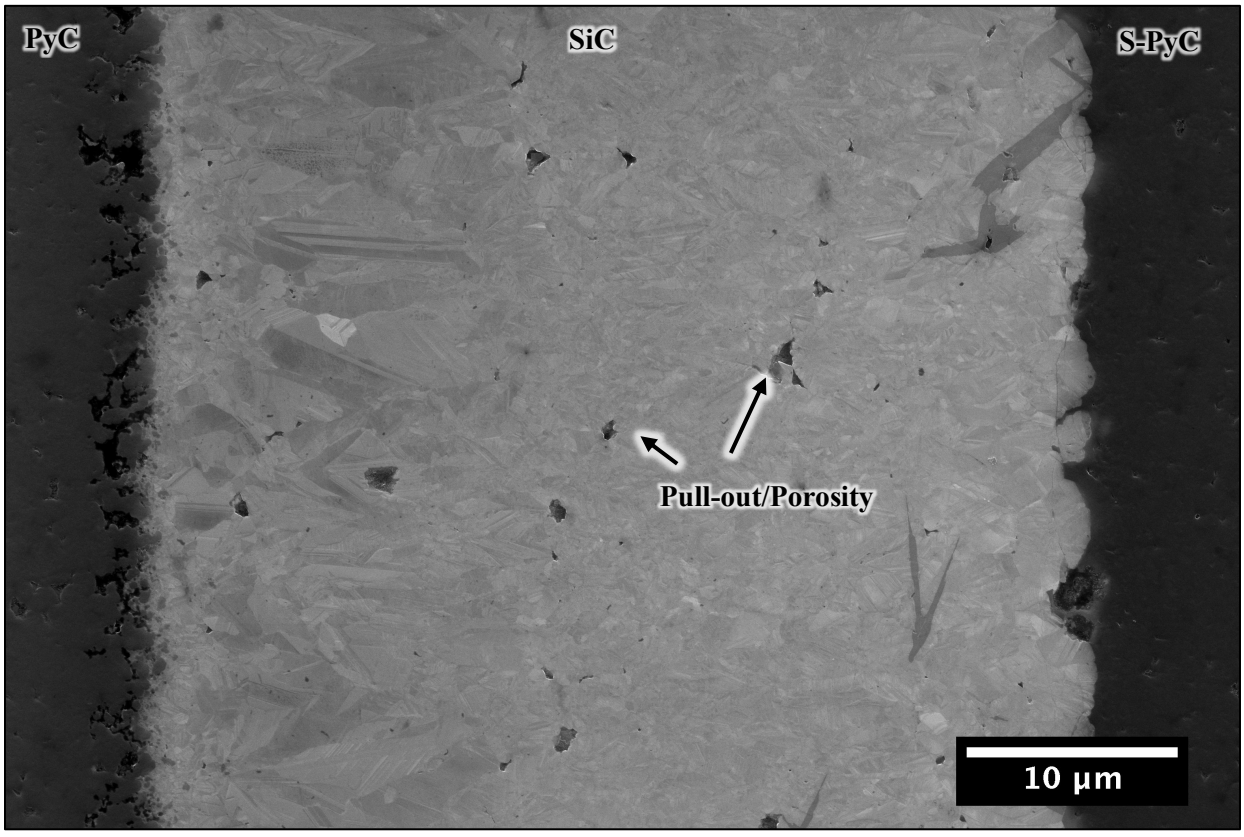

Figure 7. SEI image of DCCD-26 showing change in layer properties as a function of coating thickness.

Because of the observed disruptions in the SiC layer associated with the pure H_2 fluidization gas and high TGF required to fluidize the bed, the subsequent SiC Variant deposition, DCCD-28, revisited the Ar:H_2

fluidization approach and instead focused on increasing the deposition temperature. The DCCD-28 run was similar to DCCD-23 (Baseline and PyC Variant deposition conditions) as it used the same TGF, and CGF, however, the deposition temperature was 100 °C greater at 1550 °C. The coating run of DCCD-29 served as a comparison point, using pure H_2 fluidization gas and maintaining the same TGF and CGF, but with a higher deposition temperature (1550 °C) compared to DCCD-26. Both depositions presented larger grain sizes than the previous coating runs (Table 5). Based on the measured grain size, DCCD-28 satisfied the microstructural target for the SiC Variant, as such, it was chosen as the optimal deposition conditions. Figure 8 shows the microstructure of the SiC layer from DCCD-28; the large-grained microstructure is apparent when compared to the microstructure of the Baseline/PyC Variant (Figure 4). Also noted is the non-representative structure at the outer edge of the SiC layer near the SiC/S-PyC interface which was also observed in the Baseline and PyC Varient Ar:H_2 runs; because this is beyond the region subjected to diffusion analysis, it is not expected to influence the analysis.

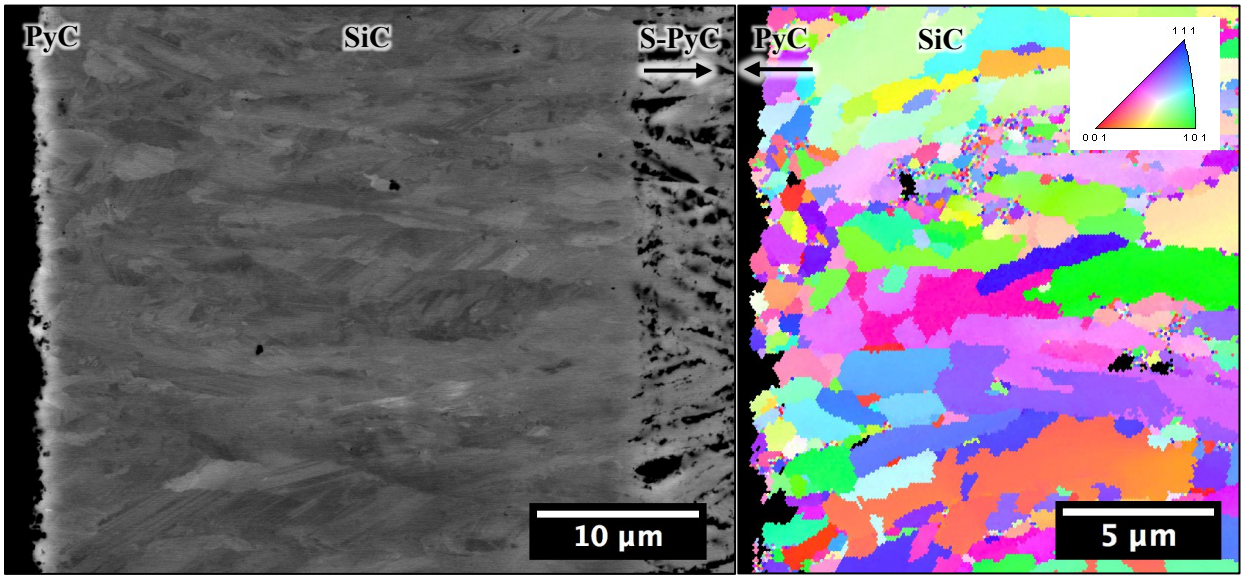

Figure 8. BSE micrograph and EBSD IPF map of the SiC layer from DCCD-28 highlighting the SiC microstructure of the SiC Variant deposition conditions.

As noted, the coating run for DCCD-29 also showed increased grain sizes, however, a significant disruption in the coating process was apparent in the mid-region of the SiC layer. Figure 9 shows a BSE image of the SiC layer for the DCCD-28 run. An obvious disruption in the coating process was observed. The cause for this disruption is not explicitly clear, however, the layer direputions are observed across multiple coating runs (Figure 7 and Figure 9) and is associated with the increased TGF with the pure H_2 fluidization gas runs. To better understand the disruptions, the PyC/SiC/S-PyC-coated ZrO_2 kernels used as fluidization media will be examined from already completed runs to understand the impact of geometry on the final microstructure.

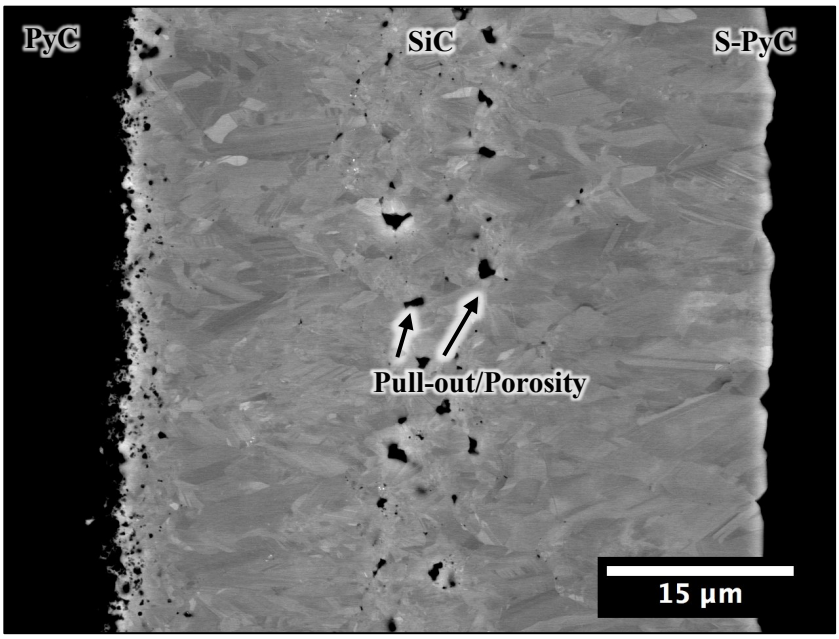

Figure 9. BSE image of the SiC layer for the DCCD-29 run showing a disruption in the SiC coating layer.

2.3 PRODUCTION OF FINAL SAMPLES

The deposition conditions have been identified for all three variants. The coating runs of DCCD-23, DCCD-27, and DCCD-30 represent full production runs for Baseline, SiC, and PyC Variants, respectively. A maximum of ~20 samples per coating run can be produced per coating run. This requires a minimum of two coating runs each to produce the needed samples for the test matrix.

3. SEAL COATING

The process for depositing a robust seal coat that provides a hermetic seal at elevated temperature was demonstrated in FY17 [1]. The coating conditions to provide an adequate SiC seal coat are listed in Table 6.

Table 6. SiC seal coating conditions.

Layer	Run Time (min)	Temp. (°C)	Ar	H_2	CGF[a]	MTS used (g)
Seal coat SiC	157	1425	3500	3500	0.023	175

All gas flow rates are in sccm.

This quarter focused on improving the efficiency of the seal coat deposition process and testing the retention of the fastest diffusion species, silver. A primary focus was on reducing the time the samples spend at temperature prior to SiC deposition. This is important as reducing the time to deposition improves the ability to retain the implanted silver in the PyC substrates. The time to initiate deposition has been refined to approximately 10 seconds.

Test samples from DCCD-06 were implanted with a Ag^+ fluence of $4.2x10^{16}$ ions/cm^2, which results in an approximate peak concentration of 5 at%. Initial seal coating tests show no indication of retained silver after seal coating via SEM-EDS analysis of a sample cross-sectional. However, the detection limits of the SEM-EDS technique is approximately 0.1 at%. The retained fraction will be ultimately determined by

Laser-induced Breakdown Spectroscopy which is in process. A diffusion barrier in being sought to impeade the loss of the implanted species from the PyC layer during SiC seal coating. No diffusion barrier layer was prefered as creating two consistent PyC/SiC interfaces was considered ideal, this approach prompted the use of the FB-CVD SiC seal coat.

The results from the seal coating trials without a diffusion barrier have prompted investigation into the application of diffusion barriers. The use of a diffusion barrier has been successfully demonstrated in Ag/SiC diffusion couples subsequently coated with SiC in a FB-CVD reactor [8]. The two approaches under investigation include low temperature techniques relative to the FB-CVD SiC deposition, which include SiC deposition via polycarbosilane precursors [8] and SiC FB-CVD deposition via methylsilane [9]. Both techniques provide opportunity to deposit a SiC layer capable of impeding release during the final SiC seal coating via the deposition route described in Table 6. The capability to deposit SiC via both routes at Oak Ridge National Laboratory have been identified and are being pursued.

4. SUMMARY

The deposition conditions necessary to meet the targeted PyC density and SiC microstructural properties have been confirmed for the three sample variants (Baseline, PyC Variant, and SiC Variant). Production of the final samples for diffusion analysis is in process. Development of a diffusion barrier to impede the loss of the mobile silver implanted dose has been initiated.

5. REFERENCES

1. Gerczak, T.J., et al., *Progress on Fabrication of Planar Diffusion Couples with Representative TRISO PyC/SiC Microstructure*. ORNL/TM-2017/704, 2017. Oak Ridge: Oak Ridge National Laboratory.
2. Collin, B.P., *AGR-1 Irradiation Test Final As-Run Report*. INL/EXT-10-18097, Revision 1, 2012. Idaho Falls: Idaho National Laboratory.
3. Collin, B.P., *AGR-2 Irradiation Test Final As-Run Report*. INL/EXT-14-32277, Revision 3, 2017. Idaho Falls: Idaho National Laboratory.
4. Gerczak, T.J., et al., *SiC layer microstructure in AGR-1 and AGR-2 TRISO fuel particles and the influence of its variation on the effective diffusion of key fission products*. Journal of Nuclear Materials, 2016. 480: p. 257-270.
5. Hunn, J.D., Measurement of PyC Density using a Density Gradient Column. AGR-CHAR-DAM-03, Revision 4, 2013. Oak Ridge: Oak Ridge National Laboratory.
6. Lowden, R.A., *Fabrication of Baseline and Variant Particle Fuel for AGR-1*. ORNL/CF-06/02, 2006. Oak Ridge: Oak Ridge National Laboratory.
7. Hunn, J.D., T.S. Byun, J.H. Miller, *Fabrication and Characterization of Sixteen SiC Variants Deposited on the Same IPyC Substrate for Fracture Strength Testing*. ORNL/TM-2009/324, 2009. Oak Ridge: Oak Ridge National Laboratory.
8. López-Honorato, E., et al., *Silver Diffusion in Coated Fuel Particles*. Journal of the American Ceramic Society, 2010. 93(10): p. 3076-3079.
9. Miller, J.H., *Methylsilane Derived SiC Particle Coatings Produced by Fluid-Bed Chemical Vapor Deposition*, Ph.D Thesis, University of Tennessee, Knoxville, December 2006.